

# Diagnostic Value of Multimodal Magnetic Resonance Imaging in Discriminating Between Metastatic and Non-Metastatic Pelvic Lymph Nodes in Cervical Cancer

Jian Xu<sup>1,\*</sup>, Yingli Ma<sup>2,\*</sup>, Haibing Mei<sup>1</sup>, Qimin Wang<sup>1</sup>

<sup>1</sup>Department of Radiology, Ningbo Women & Children's Hospital, Ningbo, People's Republic of China; <sup>2</sup>Department of Neurology, Ningbo Hospital of Traditional Chinese Medicine, Ningbo, People's Republic of China

\*These authors contributed equally to this work

Correspondence: Haibing Mei, Department of Radiology, Ningbo Women & Children's Hospital, Ningbo, People's Republic of China, Email meihbagg@163.com

**Background:** The status of pelvic lymph node (PLN) metastasis affects treatment and prognosis plans in patients with cervical cancer. However, it is hard to be diagnosed in clinical practice.

**Purpose:** The present study aimed to evaluate the diagnostic value of multimodal magnetic resonance imaging (MRI) in discriminating between metastatic and non-metastatic pelvic lymph nodes (PLNs) in cervical cancer.

**Methods:** This retrospective study analyzed MRIs of 209 PLNs in 25 women with pathologically proven cervical cancer. All PLNs had been assessed by pre-treatment multimodal MRIs, and their status was finally confirmed by histopathology. In conventional MRI, lymph node characteristics were compared between metastatic and non-metastatic PLNs. Signal intensity, time-intensity curve (TIC) patterns minimal and mean apparent diffusion coefficients (ADC) were compared between them in DWI. In DCE-MRI, quantitative ( $K_{trans}$ ,  $K_{ep}$  and  $V_e$ ) analyses were performed on DCE-MRI sequences, and their predictive values were analyzed by ROC curves.

**Results:** Of 209 PLNs, 22 (10.53%) were metastases and 187 (89.47%) were non-metastases at histopathologic examination. Considering a comparison of lymph node characteristics, the short axis size, the long axis size, and the boundary differed significantly between the two groups ( $P < 0.05$ ). The differences in  $ADC_{min}$ , TIC types,  $K_{trans}$  and  $V_e$  between metastatic and non-metastatic PLNs were significant as well ( $P < 0.05$ ). The good diagnostic performance of multimodal MRI was shown in discriminating between metastatic and non-metastatic PLNs, with the sensitivity of 85.0% (17/20), specificity of 97.3% (184/189), and accuracy of 96.2% (201/209). ROC analyses showed that the diagnostic accuracy of  $ADC_{min}$ ,  $K_{trans}$  and  $V_e$  for discriminating between metastatic and non-metastatic PLNs in cervical cancer was 83.7%, 91.4%, and 92.4% with the cut-off values of  $0.72 \times 10^{-3} \text{ mm}^2/\text{s}$ ,  $0.52 \text{ min}^{-1}$ , and  $0.53 \text{ min}^{-1}$ , respectively.

**Conclusion:** Multimodal MRI showed good diagnostic performance in determining PLN status in cervical cancer.

**Keywords:** multimodal magnetic resonance imaging, cervical cancer, lymphatic metastasis, apparent diffusion coefficient

## Introduction

Cervical cancer is the fourth leading cause of cancer-related mortality in women worldwide.<sup>1</sup> The extent of pelvic lymph node (PLN) metastasis is an important prognostic factor, and the survival rates of patients with PLN metastasis are significantly lower than those of patients without such metastasis. PLN metastasis also affects the initial treatment strategy for cervical cancer and is hard to be diagnosed in clinical practice. At present, treatment and prognosis plans for patients with cervical cancer are mainly based on the Federation International of Gynecology and Obstetrics (FIGO) stage. According to FIGO 2018 for cervical cancer, regardless of tumor size and parametrial infiltration, the involvement

of lymph node metastasis is classified as stage IIIC.<sup>2</sup> Therefore, evaluating the status of PLN is crucial in staging, developing individualized treatment plans, and improving prognosis in cervical cancer.

In this regard, magnetic resonance imaging (MRI) with superior soft-tissue resolution is widely used in detecting metastatic lymph nodes. However, MRI is mainly based on measurements of node size and morphologic information and yielded inadequate results for diagnosis. Diffusion weighted imaging (DWI) has significantly increased the value and accuracy of MRI. The DWI technique provides molecular tissue diffusion and can accurately detect local metastasis in tumors with high precision.<sup>3</sup> However, not enough evidence was available to support the fact that DWI could independently characterize a pelvic mass.<sup>4</sup> In dynamic contrast enhanced (DCE)-MRI, tissue enhancement is evaluated according to the time. This method is more accurate than conventional contrast enhanced MRI and could differentiate between metastatic and non-metastatic lesions on the basis of the differences in their enhancement parameters.<sup>5</sup>

A multimodal MRI approach that incorporates conventional MRI, DWI and DCE-MRI yields significant improvement in accuracy over each modality separately in tumor detection and characterization. Recently, increasing attempts have been made to test the diagnostic accuracy of multimodal MRI in predicting lymph node metastases. To date, there is a paucity of information in the literature about the diagnostic value of multimodal MRI in determining pelvic lymph node status in patients with cervical cancer. The present study aimed to investigate the value of multimodal MRI and its quantitative parameters in discriminating between metastatic and non-metastatic PLNs in patients with cervical cancer.

## Methods

### Participants

This study was approved by the Clinical Ethics Committee of Ningbo Women & Children's Hospital. This study complied with the Declaration of Helsinki. All participants provided written informed consent prior to the MRI exam. Twenty-five untreated patients with cervical cancer aged 35-62 years were consecutively evaluated at our hospital from January 2019 to August 2021. All PLNs in 25 patients had been assessed by pretreatment multimodal MRI and their status was finally confirmed by histopathology. Exclusion criteria were primary pelvic disease, and the existence of metal anywhere in the body. Besides, patients who underwent radiotherapy or chemotherapy were also excluded in our study.

### MRI Technique

MRI data were acquired using a 1.5 T superconducting magnetic resonance system (Achieva 1.5 T Nova Dual, Philips Healthcare, Best, Netherlands) equipped with a dedicated 16-channel phased array torso coil. The area of interest was the whole pelvis, scanning from perineum up to the fifth lumbar. T1-weighted (T1W) gradient echo images were obtained using the following parameters: repetition time (TR)=490ms, echo time (TE)=80ms, flip angle=10 degrees. T2-weighted (T2W) single-shot turbo spin echo images were collected using the following parameters: TR=3500ms, TE=80ms, echo train length (ETL)=19. T2Wfat-suppressed spin echo images were obtained using the following settings: TR=3275ms, TE=80ms, ETL=22. DWI was obtained in the axial plane using a multi-slice spin echo planar imaging (EPI) sequence. Imaging parameters were as follows: TR=1118ms, TE=60ms, TI=180ms. DWI was acquired with diffusion-weighted b factor of 0 and 800 seconds/mm<sup>2</sup>, and apparent diffusion coefficient (ADC) maps were generated for all images. After the acquisition of DWIs, DCE images acquisition was performed using T1 high resolution isotropic volume examination (THRIVE) sequences with the following parameters: TR=3.4ms, TE=1.6ms, field of view (FOV)= 240mm×192mm, matrix= 256×192, slice thickness= 4mm. Dynamic technique was performed at 32 time phases with a frequency-selective pre-saturation pulse using intravenous injection of 0.1 mmol/kg gadodiamide at a rate of 3 mL/minute at the third time phase for all patients.

### Image Analysis

All images were reviewed independently on the Philips workstation by two experienced radiologists in gynecologic radiology. The reviewers were blinded to the histology. The region of interest (ROI) was placed to include the target lesion on the ADC map and exclude the necrotic or hemorrhagic areas in the PLNs according to T1WI and T2WI. Area of ROI was no less than 50 mm<sup>2</sup>. Time-intensity curves (TICs) were produced for the lesions by Omni-Kinetics software on the Philips workstation. TIC patterns were categorized as follows:<sup>6</sup> Type I was defined as a mildly persistent gradual

increase without a shoulder, Type II as a moderate initial increase followed by a plateau and Type III as a relatively rapid uptake followed by reduction in enhancement towards the latter part of the study. The transfer constant ( $K_{trans}$ ), rate constant ( $K_{ep}$ ), and extravascular extracellular volume fraction ( $V_e$ ) were calculated using a pharmacokinetic model. Short-axis and long-axis diameters of each identifiable node were measured on axial images using electronic calipers, and the long-to-short axis ratio was calculated.

## Statistical Analysis

The mean quantitative data were presented as average  $\pm$  standard deviation, and the qualitative variables were expressed as proportion (percentage). The normality assumption of continuous data was evaluated using the *Kolmogorov–Smirnov* test. A *Chi-square* test was conducted to compare the qualitative variables between metastatic and non-metastatic lymph nodes. Independent sample *t* test was used to compare the ADC values,  $K_{trans}$ ,  $K_{ep}$  and  $V_e$  between the metastatic and non-metastatic pelvic lymph nodes. Receiver operating characteristic (ROC) curves were performed for assessing the efficacy of ADC value,  $K_{trans}$  and  $K_{ep}$  in the identification of metastatic PLNs. All statistical analyses were performed using SPSS 22.0 (SPSS, IBM, Somers, NY). A level of  $P < 0.05$  was considered to be statistically significant.

## Results

### Comparisons of Conventional MRI Metrics Between Metastatic and Non-Metastatic PLNs in Cervical Cancer

Of 209 PLNs, 22 (10.53%) were metastases and 187 (89.47%) were non-metastases at histopathologic examination (Figure 1). Table 1 lists a comparison of the lymph node characteristics between metastatic and non-metastatic PLNs in cervical cancer. The mean size of long axis of metastatic and non-metastatic PLNs is  $11.30 \pm 6.62$  mm and  $7.85 \pm 2.08$  mm, respectively. The mean size of short axis of metastatic and non-metastatic PLNs is  $7.25 \pm 3.31$  mm and  $5.52 \pm 0.95$  mm, respectively. In the assessment of the boundary, 77.27% (17/22) of metastatic and 99.47% (186/187) of non-metastatic PLNs were well-delineated. All of the above examined variables differed significantly between the two study groups ( $P < 0.001$ ).

### Comparisons of DWI Metrics Between Metastatic and Non-Metastatic PLNs

No significant difference was observed between metastatic and non-metastatic PLNs in terms of signal intensity ratios in T1WI. The difference in the values of ADC map between metastatic and non-metastatic PLNs was significant ( $P < 0.001$ ). Concerning the evaluation of TIC types, a statistically significant difference was detected between metastatic and non-metastatic PLNs ( $P < 0.001$ ). The minimum and mean values of ADC metrics were evaluated between metastatic and non-metastatic PLNs as well. These indicated a significantly lower  $ADC_{min}$  in those with metastatic PLNs than those with non-metastatic PLNs. No significant difference was observed between metastatic and non-metastatic PLNs in the value of  $ADC_{mean}$  (Table 1 and Figure 2).

### Comparisons of DCE-MRI Metrics Between Metastatic and Non-Metastatic PLNs

The values of  $K_{trans}$  and  $V_e$  were significantly higher in those with metastatic PLNs than those with non-metastatic PLNs ( $P < 0.001$ ). There were no significant differences between values of  $K_{ep}$  between the two groups (Table 1 and Figure 2).

### Comparisons of Characteristics Between True-Positive and False-Positive, Between True-Negative and False-Negative PLNs

According to histopathologic review, there were five false-positive and three false-negative PLNs (Figure 1). We then compared the values of characteristics between true-positive ( $n = 17$ ) and false-positive ( $n = 5$ ), between true-negative ( $n = 184$ ) and false-negative ( $n = 3$ ) PLNs, respectively. No significant difference was observed in the short axis size between true-negative and false-negative PLNs ( $P > 0.05$ ). There were also no significant differences between true-positive and false-positive, between true-negative and false-negative PLNs in terms of the long axis size, the long to short axis ratio, and

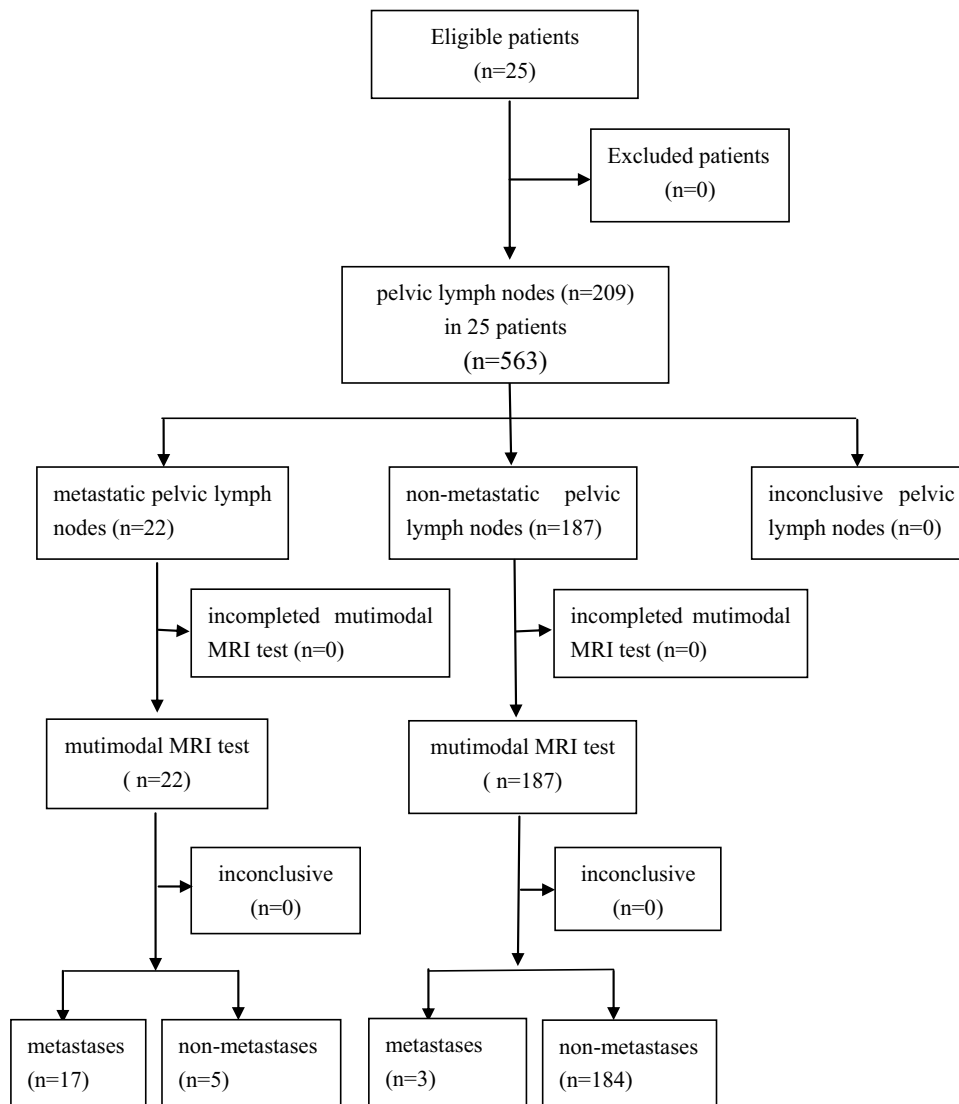


**Figure 1** STARD flow diagram of multimodal MRI in discriminating between metastatic and non-metastatic pelvic lymph nodes in 25 patients with cervical cancer.

boundary ( $P>0.05$ ). As shown in Figures 3–5, significant differences were observed between true-positive and false-positive, between true-negative and false-negative PLNs in the values of  $ADC_{min}$ ,  $K_{trans}$ , and  $V_e$ , respectively ( $P<0.05$ ).

### ROC Analysis of $ADC_{min}$ , $K_{trans}$ and $V_e$ in Discriminating Between Metastatic and Non-Metastatic PLNs

The present study demonstrated the good diagnostic performance of multimodal MRI in discriminating between metastatic and non-metastatic PLNs in cervical cancer, with the sensitivity of 85.0% (17/20), specificity of 97.3% (184/189), and accuracy of 96.2% (201/209). ROC analysis was used to determine the diagnostic performance and the cut-off values of  $ADC_{min}$ ,  $K_{trans}$  and  $V_e$  for discriminating between metastatic and non-metastatic PLNs in cervical cancer. When the  $ADC_{min}$  value of  $0.72 \times 10^{-3} \text{mm}^2/\text{s}$  was used as a cut-off value, the best validity results were obtained, with sensitivity of 83.1%, specificity of 89.6%, and accuracy of 83.7%. The cut-off value of  $K_{trans}$  was set at  $0.52 \text{min}^{-1}$  for discriminating between metastatic and non-metastatic PLNs in cervical cancer, with sensitivity of 90.3%, specificity of 96.5%, and accuracy of 91.4%. The cut-off value of  $V_e$  was set at  $0.53 \text{min}^{-1}$ , with sensitivity of 89.3%, specificity of 98.2%, and accuracy of 92.4%. Figure 6 displays the ROC analysis of  $ADC_{min}$ ,  $K_{trans}$  and  $V_e$  in discriminating between metastatic and non-metastatic PLNs in cervical cancer.

**Table 1** Characteristics of Non-Metastatic and Metastatic PLNs in Cervical Cancer

Variables	Metastasized (n=22)	Non-Metastasized (n=187)	P-value
Long axis size (mm)	11.30±6.62	7.85±2.08	<b>0.023</b>
Short axis size (mm)	7.25±3.31	5.52±0.95	<b>0.024</b>
Long to short axis size (mm)	1.52±0.32	1.43±0.30	0.201
Boundary			<b>&lt;0.001</b>
Clear	17 (77.27%)	186 (99.47%)	
Unclear	5 (22.72%)	1 (0.53%)	
T1WI			0.313
Hyperintense	12 (45.45%)	87 (46.52%)	
Isointense	10 (54.54%)	100 (53.48%)	
T2WI			0.609
Hyperintense	19 (86.36%)	160 (85.56%)	
Isointense	3 (13.64%)	27 (14.44%)	
ADC map			<b>&lt;0.001</b>
Hyper/isointense	2 (9.09%)	166 (88.77%)	
Hypointense	20 (90.91%)	21 (11.23%)	
TIC types			<b>&lt;0.001</b>
I	1 (4.55%)	165 (88.24%)	
II	18 (81.82%)	22 (11.76%)	
III	3 (13.63%)	0 (0%)	
ADC <sub>min</sub> (×10 <sup>-3</sup> mm/s)	0.63±0.14	0.86±0.44	<b>&lt;0.001</b>
ADC <sub>mean</sub> (×10 <sup>-3</sup> mm/s)	1.06±0.38	0.99±0.30	0.393
K <sub>trans</sub> (min <sup>-1</sup> )	0.63±0.14	0.39±0.16	<b>&lt;0.001</b>
K <sub>ep</sub> (min <sup>-1</sup> )	1.20±0.55	1.04±0.82	0.239
V <sub>e</sub>	0.59±0.19	0.49±0.21	<b>0.035</b>

**Notes:** P values are marked in bold text if they are below 0.05.

**Abbreviations:** PLNs, pelvic lymph nodes; T1WI, T1-weighted imaging; T2WI, T2-weighted imaging; ADC, apparent diffusion coefficient; TIC, time-intensity curve; K<sub>trans</sub>, transfer constant; K<sub>ep</sub>, rate constant; V<sub>e</sub>, extravascular extracellular volume.

## Discussion

Discriminating between metastatic and non-metastatic PLNs in cervical cancer is useful for diagnosing the stage and determining therapeutic strategies. A multimodal MRI approach that incorporates conventional MRI, DWI and DCE-MRI has been widely used in determining its metastasis, especially in the preoperative stages. However, the precision of this approach in PLNs in patients with cervical cancer remains unclear. The present study demonstrated the good diagnostic performance of multimodal MRI in discriminating between metastatic and non-metastatic PLNs in cervical cancer, with the sensitivity of 85.0%, specificity of 97.3%, and accuracy of 93.3%. Different values of the ADC<sub>min</sub>, K<sub>trans</sub> and V<sub>e</sub>, could effectively predict lymph node metastasis with high sensitivity and specificity. The optimal cut-off values of ADC<sub>min</sub>, K<sub>trans</sub> and V<sub>e</sub> in discriminating between metastatic and non-metastatic PLNs in patients with cervical cancer were  $0.72 \times 10^{-3} \text{mm}^2/\text{s}$ ,  $0.52 \text{min}^{-1}$ , and  $0.53 \text{min}^{-1}$ , respectively.

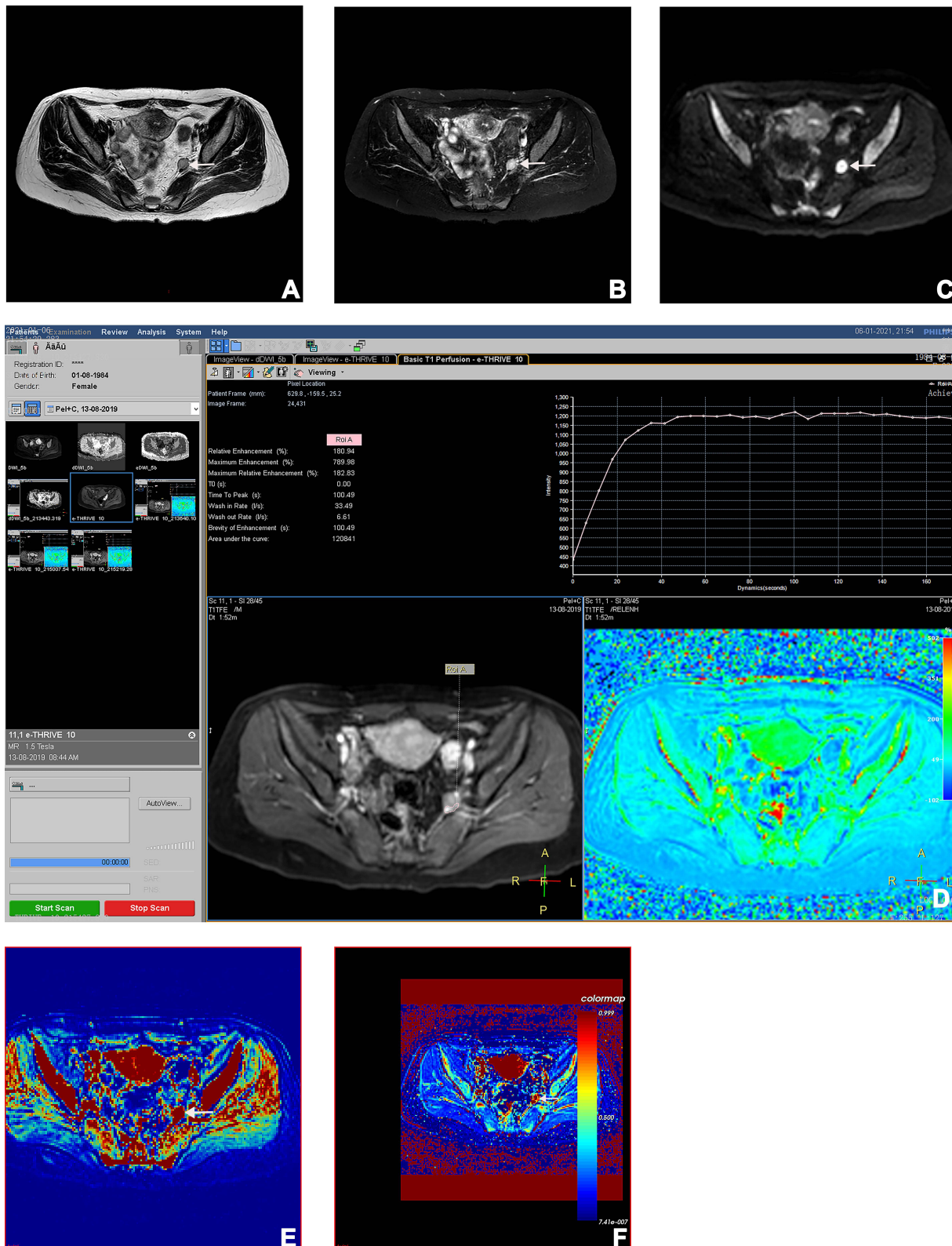


**Figure 2** A 58-year-old woman with cervical cancer. (A) AxialT1WI shows a metastatic pelvic lymph node with hyperintense (white arrow). (B) Axial DWI shows a metastatic pelvic lymph node with hyperintense (white arrow). (C) Axial T2WI SPAIR shows a metastatic pelvic lymph node with hyperintense (white arrow). (D) Axial DWI shows a metastatic pelvic lymph node presented in TIC type III. (E) Image of  $K_{trans}$  shows a metastatic pelvic lymph node in warm color (white arrow). (F) Image of  $V_{le}$  shows a metastatic pelvic lymph node in warm color (white arrow).

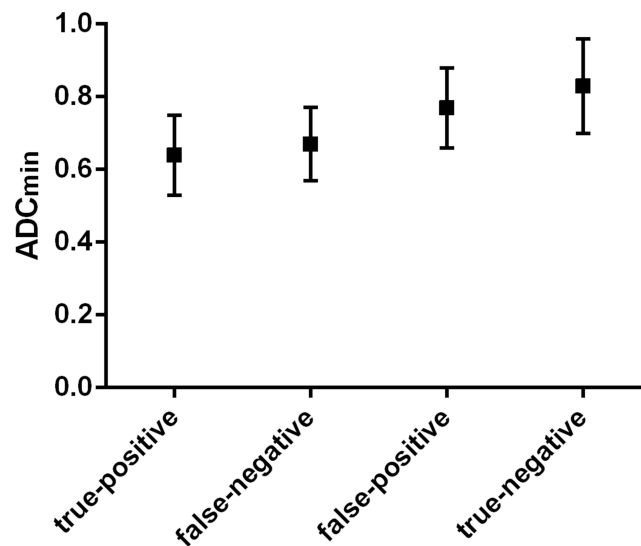


**Figure 3** Box and whisker plot comparing the minimum value of ADC of true-positive, false-negative, false-positive, true-negative pelvic lymph nodes diagnosed by multimodal MRI.

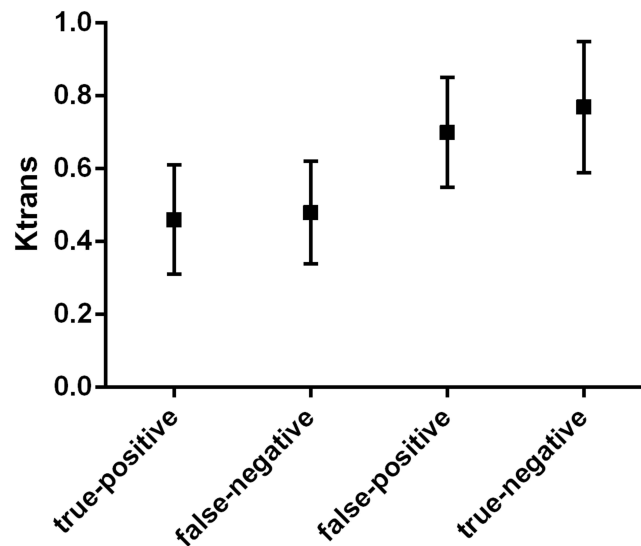


**Figure 4** Box and whisker plot comparing the value of  $K_{trans}$  of true-positive, false-negative, false-positive, true-negative pelvic lymph nodes diagnosed by multimodal MRI.

Conventional MRI is mainly based on measurements of node size and morphologic information and yields low sensitivity in detecting lymph node metastasis. The sensitivity of conventional MRI in distinguishing metastatic PLNs from non-metastatic ones in patients with cervical cancer was ranging from 30.3% to 72.9%,<sup>7,8</sup> which remains to be improved. Computed tomography (CT) is widely used in the diagnosis of cervical cancer, but it is less effective in determining distant lymph node metastasis.<sup>9</sup> Benefit from advances in molecular imaging technology, multimodal MRI is particularly crucial in the diagnosis, staging, and prognostic evaluation of malignant tumors. Liu et al<sup>10</sup> reported that multimodal MRI can have essential clinical value in the differentiation between brain metastases and high-grade gliomas.

DWI reflects the Brownian movement of water in living tissues by imaging diffusion characteristics. It is sensitive to the diffusion of water molecules in tissue, which can make subtle abnormality more obvious and can provide better characterization of tissue and their pathological processes at microscopic level.<sup>11</sup> Additionally, the quantitative assessment can be performed by the measurement of the ADC values.<sup>12</sup> DWI has been reported to be capable of distinguishing metastatic from non-metastatic PLNs in patients with cervical cancer. Chen et al<sup>13</sup> reported that DWI with ADC

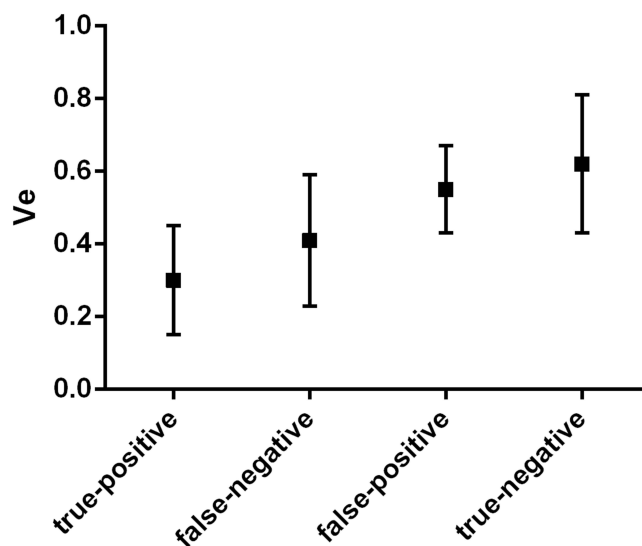


**Figure 5** Box and whisker plot comparing the value of  $V_e$  of true-positive, false-negative, false-positive, true-negative pelvic lymph nodes diagnosed by multimodal MRI.

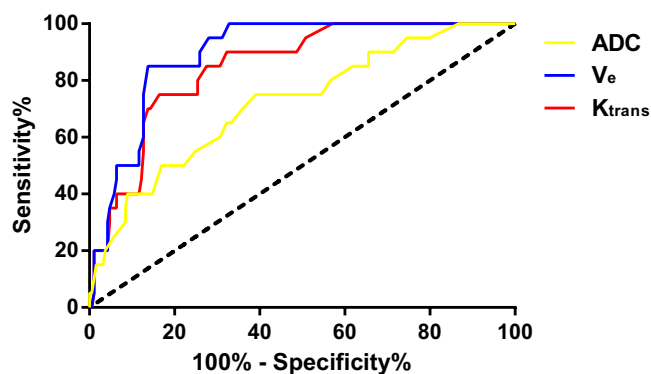


**Figure 6** ROC curves of  $ADC_{min}$ ,  $K_{trans}$  and  $V_e$  in discriminating between metastatic and non-metastatic PLNs in cervical cancer.

measurements could differentiate metastatic from hyperplastic nodes with a sensitivity of 83.3%, specificity of 74.7% and accuracy of 78.4%. In the present study, a significantly lower  $ADC_{min}$  was observed in those with metastatic PLNs than those with non-metastatic PLNs. When the  $ADC_{min}$  value of  $0.72 \times 10^{-3} \text{mm}^2/\text{s}$  was used as a cut-off value, the best validity results were obtained, with the sensitivity of 83.1%, specificity of 89.6%, and accuracy of 83.7%. These results were consistent with the previous study by Zhang et al.<sup>14</sup> Nevertheless, using DWI alone is not accurate enough to rule in or out PLN metastases.

DCE-MRI for characterizing tissue uptake of a paramagnetic contrast agent is a non-invasive imaging method for assessing microcirculation physiology in normal and diseased tissue. Although DCE-MRI provides quantitative analysis of tumor vascular permeability, the accuracy of some parameters in PLNs remains unclear. Quantitative parameters directly related to underlying physiological properties, such as  $K_{trans}$ ,  $K_{ep}$  and  $V_e$ .<sup>15</sup>  $K_{trans}$  represents the volume transfer constant of the contrast agent from vascular space (VS) to extra-vascular extracellular space (EES).  $K_{ep}$  represents the rate of reverse transfer constant of the contrast agent to VS, and  $V_e$  represents the volume of EES per unit volume of the contrast agent in the tissue.  $K_{trans}$  and  $V_e$  parameters reflect perfusion and permeability, the reverse transportation of contrast agent back to the VS as well as EES. In the present study, the values of  $K_{trans}$  and  $V_e$  were significantly higher in those with metastatic PLNs than those with non-metastatic PLNs. There were no significant differences between the values of  $K_{ep}$  between the two groups. TIC can intuitively and quantitatively reflect the characteristics of tumor and lymph node enhancement. The method was described by Kuhl et al.<sup>16</sup> and they concluded that the type III time-course is

a strong predictor of malignancy. In this study, the difference in TIC types between metastatic and non-metastatic PLNs was statistically significant ( $P < 0.05$ ). Moreover, 81.81% (18/22) of PLNs that presented type III were pathologically proven malignancy. These results were in accordance with the study by Kuhl et al.<sup>16</sup>

Interestingly, there were five false-positive and three false-negative PLNs scanned by multimodal MRI. We tried to explain the reason for this false MRI diagnosis by comparing characteristics between true-positive and false-positive, between true-negative and false-negative PLNs, respectively. We found that a considerable overlap of the values of characteristics among true-positive, false-positive, true-negative, and false-negative PLNs contributed to false MRI diagnosis. This was consistent with previous studies.<sup>17,18</sup> The size of lymph node is a standard criterion for predicting lymph node involvement. Although metastatic lymph nodes usually have a larger short-axis diameter than non-metastatic lymph nodes, approximately 30% of metastatic lymph nodes have a diameter of smaller than 4 mm.<sup>19</sup> In addition, non-metastatic lymph nodes may appear to increase in size with the development of fibrosis.<sup>20</sup> Besides, certain types of inflammation tend to present with a dense fibrous reactions, thereby impeding diffusion and lowering ADC values, leading to false-positive results.<sup>21</sup> It is difficult and challenging to address the issue of false diagnosis of PLNs by human beings. In the future, artificial intelligence is expected to become an optimal option for reducing false MRI diagnosis of PLNs in patients with cervical cancer.

This study has several limitations. First, this was a retrospective, single-centre study with a relatively small sample size. The methods we evaluated should be conducted on a large sample population to yield more accurate estimates of their diagnostic characteristics. Moreover, the costs and availability of a diagnostic test is also an important factor that should be considered in choosing the best method.

## Conclusion

Multimodal MRI showed good diagnostic performance in determining PLN status in patients with cervical cancer. The methods proposed herein may aid the determination of metastatic PLNs in a non-invasive manner and provide a systematic imaging basis for clinical practice.

## Disclosure

The authors declare that there are no conflicts of interest.

## References

1. Cohen PA, Jhingran A, Oaknin A, Denny L. Cervical cancer. *Lancet*. 2019;393(10167):169–182.
2. Matsuo K, Machida H, Mandelbaum RS, Konishi I, Mikami M. Validation of the 2018 FIGO cervical cancer staging system. *Gynecol Oncol*. 2019;152(1):87–93.
3. Tang L, Zhou XJ. Diffusion MRI of cancer: from low to high b-values. *J Magnetic Resonance Imaging*. 2019;49(1):23–40.
4. Thomassin-Naggara I, Bazot M, Daraï E, Callard P, Thomassin J, Cuenod CA. Epithelial ovarian tumors: value of dynamic contrast-enhanced MR imaging and correlation with tumor angiogenesis. *Radiology*. 2008;248(1):148–159.
5. Yan Y, Sun X, Shen B. Contrast agents in dynamic contrast-enhanced magnetic resonance imaging. *Oncotarget*. 2017;8(26):43491–43505.
6. Thomassin-Naggara I, Balvay D, Rockall A, et al. Added value of assessing adnexal masses with advanced MRI techniques. *Biomed Res Int*. 2015;2015:785206.
7. Liu B, Gao S, Li S, Comprehensive A. Comparison of CT, MRI, Positron emission tomography or positron emission tomography/CT, and diffusion weighted imaging-MRI for detecting the lymph nodes metastases in patients with cervical cancer: a meta-analysis based on 67 studies. *Gynecol Obstet Invest*. 2017;82(3):209–222.
8. Choi HJ, Ju W, Myung SK, Kim Y. Diagnostic performance of computer tomography, magnetic resonance imaging, and positron emission tomography or positron emission tomography/computer tomography for detection of metastatic lymph nodes in patients with cervical cancer: meta-analysis. *Cancer Sci*. 2010;101(6):1471–1479.
9. Dag Z, Yilmaz B, Dogan AK, et al. Comparison of the prognostic value of F-18 FDG PET/CT metabolic parameters of primary tumors and MRI findings in patients with locally advanced cervical cancer treated with concurrent chemoradiotherapy. *Brachytherapy*. 2019;18(2):154–162.
10. Liu J, Han H, Xu Y, et al. A comparison of the multimodal magnetic resonance imaging features of brain metastases vs. high-grade gliomas. *Am J Transl Res*. 2021;13(4):3543–3548.
11. Abdel Razek AA, Soliman NY, Elkhamary S, Alsharaway MK, Tawfik A. Role of diffusion-weighted MR imaging in cervical lymphadenopathy. *Eur Radiol*. 2006;16(7):1468–1477.
12. Koc Z, Erbay G, Ulsan S, Seydaoglu G, Aka-Bolat F. Optimization of b value in diffusion-weighted MRI for characterization of benign and malignant gynecological lesions. *J Magnetic Resonance Imaging*. 2012;35(3):650–659.
13. Chen YB, Liao J, Xie R, Chen GL, Chen G. Discrimination of metastatic from hyperplastic pelvic lymph nodes in patients with cervical cancer by diffusion-weighted magnetic resonance imaging. *Abdom Imaging*. 2011;36(1):102–109.

14. Zhang A, Song J, Ma Z, Chen T. Application of apparent diffusion coefficient values derived from diffusion-weighted imaging for assessing different sized metastatic lymph nodes in cervical cancers. *Acta Radiologica*. 2020;61(6):848–855.
15. Tofts PS. Modeling tracer kinetics in dynamic Gd-DTPA MR imaging. *J Magnetic Resonance Imaging*. 1997;7(1):91–101.
16. Kuhl CK, Mielcareck P, Klaschik S, et al. Dynamic breast MR imaging: are signal intensity time course data useful for differential diagnosis of enhancing lesions? *Radiology*. 1999;211(1):101–110.
17. Knijn N, van Erning FN, Overbeek LI, et al. Limited effect of lymph node status on the metastatic pattern in colorectal cancer. *Oncotarget*. 2016;7(22):31699–31707.
18. Yang X, Chen Y, Wen Z, et al. Role of Quantitative Dynamic Contrast-Enhanced MRI in Evaluating Regional Lymph Nodes With a Short-Axis Diameter of Less Than 5 mm in Rectal Cancer. *AJR Am J Roentgenol*. 2019;212(1):77–83.
19. Langman G, Patel A, Bowley DM. Size and distribution of lymph nodes in rectal cancer resection specimens. *Dis Colon Rectum*. 2015;58(4):406–414.
20. Nahas SC, Nahas CSR, Cama GM, et al. Diagnostic performance of magnetic resonance to assess treatment response after neoadjuvant therapy in patients with locally advanced rectal cancer. *Abdominal Radiol*. 2019;44(11):3632–3640.
21. Muenzel D, Duetsch S, Fauser C, et al. Diffusion-weighted magnetic resonance imaging in cervical lymphadenopathy: report of three cases of patients with Bartonella henselae infection mimicking malignant disease. *Acta Radiol*. 2009;50(8):914–916.

International Journal of General Medicine

Dovepress

## Publish your work in this journal

The International Journal of General Medicine is an international, peer-reviewed open-access journal that focuses on general and internal medicine, pathogenesis, epidemiology, diagnosis, monitoring and treatment protocols. The journal is characterized by the rapid reporting of reviews, original research and clinical studies across all disease areas. The manuscript management system is completely online and includes a very quick and fair peer-review system, which is all easy to use. Visit <http://www.dovepress.com/testimonials.php> to read real quotes from published authors.

Submit your manuscript here: <https://www.dovepress.com/international-journal-of-general-medicine-journal>